S.-I. Murtada
Department of Biomedical Engineering,
Yale University,
New Haven, CT 06520;
Department of Physiology and Pharmacology,
Karolinska Institutet,
Stockholm 17177, Sweden
e-mail: sae-il.murtada@yale.edu

J. Ferruzzi
Department of Biomedical Engineering,
Yale University,
New Haven, CT 06520
e-mail: jacopo.ferruzzi@yale.edu

H. Yanagisawa
Life Science Center,
Tsukuba Advanced Research Alliance,
University of Tsukuba,
Ibaraki 305-8577, Japan
e-mail: hkyanagisawa@tara.tsukuba.ac.jp

J. D. Humphrey[1]
Fellow ASME
Department of Biomedical Engineering,
Yale University,
New Haven, CT 06520
e-mail: jay.humphrey@yale.edu

Reduced Biaxial Contractility in the Descending Thoracic Aorta of Fibulin-5 Deficient Mice

The precise role of smooth muscle cell contractility in elastic arteries remains unclear, but accumulating evidence suggests that smooth muscle dysfunction plays an important role in the development of thoracic aortic aneurysms and dissections (TAADs). Given the increasing availability of mouse models of these conditions, there is a special opportunity to study roles of contractility ex vivo in intact vessels subjected to different mechanical loads. In parallel, of course, there is a similar need to study smooth muscle contractility in models that do not predispose to TAADs, particularly in cases where disease might be expected. Multiple mouse models having compromised glycoproteins that normally associate with elastin to form medial elastic fibers present with TAADs, yet those with fibulin-5 deficiency do not. In this paper, we show that deletion of the fibulin-5 gene results in a significantly diminished contractility of the thoracic aorta in response to potassium loading despite otherwise preserved characteristic active behaviors, including axial force generation and rates of contraction and relaxation. Interestingly, this diminished response manifests around an altered passive state that is defined primarily by a reduced in vivo axial stretch. Given this significant coupling between passive and active properties, a lack of significant changes in passive material stiffness may help to offset the diminished contractility and thereby protect the wall from detrimental mechanosensing and its sequelae. [DOI: 10.1115/1.4032938]

Keywords: wall mechanics, smooth muscle, active stress, passive stress, artery

Introduction

Fibulin-5 is an elastin-associated glycoprotein that is fundamental to elastogenesis in elastic arteries. The gross vascular phenotype exhibited by mice with a germline deletion of the *Fbln5* gene includes elongated and tortuous elastic arteries [1]. Detailed studies of passive aortic properties in both young [2] and mature [3] $Fbln5^{-/-}$ mice reveal further that the structural, but not material, stiffness is elevated in these mice, with altered wall mechanics manifesting similarly across different thoracic and abdominal regions independent of sex. Interestingly, $Fbln5^{-/-}$ mice do not develop TAADs, even under induced hypertension (unpublished results), while other mouse models of compromised elastin-associated glycoproteins often present with dramatic thoracic lesions [4,5]. Given that decreased expression of fibulin-5 has been reported to associate with thoracic aortic dissections in rare cases in humans [6], determining why $Fbln5^{-/-}$ mice do not develop these potentially lethal conditions could motivate new hypotheses on the development of TAADs.

It has recently been suggested that the constellation of genetic mutations that predispose to TAADs implicates a dysfunctional mechanosensing and mechanoregulation of extracellular matrix by intramural cells, especially smooth muscle cells (SMCs) [7]. These cellular functions depend on actomyosin interactions and downstream signaling pathways that overlap with those involved in vessel level vasoactivity [8,9]. There is a strong motivation, therefore, to study SMC contractility in mouse models of TAADs as well as those that unexpectedly do not lead to these lesions. In this paper, we present the first detailed study of the biaxial (circumferential and axial) contractility of the thoracic aorta in the $Fbln5^{-/-}$ mouse model. These results are compared with those for littermate $Fbln5^{+/+}$ control aortas.

Methods

Specimen Preparation. All animal protocols were approved by the Institutional Animal Care and Use Committee of Yale University. Male mice at 22 weeks of age were divided into two groups: control ($Fbln5^{+/+}$) and fibulin-5 deficient ($Fbln5^{-/-}$) that were obtained by breeding heterozygous ($Fbln5^{+/-}$) pairs that were generated on a mixed C57BL/6 × 129/SvEv background [1]. Following euthanasia induced by an intraperitoneal injection of Beuthanasia-D (150 mg/kg), the descending thoracic aorta (DTA) was harvested from the left-subclavian artery to the fifth pair of intercostal branches. The excised aortic segments were prepared immediately for biomechanical testing as described previously [10]. Briefly, following gentle removal of perivascular tissue, the specimens were cannulated on custom glass micropipettes, proximally near the first pair of intercostal branches and distally just after the fourth pair of intercostal branches, then secured with proximal and distal ligatures, and placed in an organ bath containing a Krebs-Ringer bicarbonate buffered solution at 37 °C that was bubbled with 95% O_2 and 5% CO_2 to maintain a pH of 7.4.

Testing System and Protocols. The cannulated specimens were subjected to multiple levels of static biaxial loading using a custom computer-controlled testing system [11]. Whereas the original system allows online measurement of outer diameter, distending pressure, and changes in axial length and force, an optical coherence tomography (OCT) system (Callisto model, Thorlabs, Newton, NJ) was added to measure wall thickness (with axial (depth) resolution of <7 μm and lateral resolution of 8 μm) at multiple times during testing, typically 0, 5, 10, and 15 min after inducing SMC contraction. Wall thickness and outer diameter were measured within the central region of the specimen, between the second and third pair of intercostal branches. Axial force and luminal pressure were measured with standard transducers and yielded values relevant to the central region.

[1]Corresponding author.
Manuscript received September 21, 2015; final manuscript received February 17, 2016; published online March 30, 2016. Assoc. Editor: Jonathan Vande Geest.

To ensure vessel viability and to precondition the activated smooth muscle at low loads, initial contractions were induced by increasing the potassium chloride (KCl) to 80 mM in the bathing solution with the distending pressure set at 40, then 60, mmHg at axial stretches of 1.10, then 1.20, relative to the unloaded resting length. Axial stretch was increased in increments of 0.02 and pressure was increased in increments of 5 mmHg, both to avoid any sudden large deformations in the contracted specimens. Following this preconditioning, the specimens were then contracted for 15 min at nine different combinations of constant pressure and axial stretch: the three pressures were 70, 90, and 110 mmHg whereas the three axial stretches depended on genotype, namely, $\lambda_z = 1.40-1.45$, 1.50, and 1.60 for *Fbln5*$^{+/+}$ or $\lambda_z = 1.25$, 1.30, and 1.35 for *Fbln5*$^{-/-}$. Motivation for these values of axial stretch is discussed further below, but was based largely on reported values of preferred passive axial stretches for the DTAs of 1.50 for *Fbln5*$^{+/+}$ mice and 1.39 for *Fbln5*$^{-/-}$ mice [3]. The specimens were contracted at each of these nine combinations of pressure and axial stretch via a protocol that consisted of three steps: (1) equilibrate the specimen at the prescribed pressure and axial stretch for 5 min in the normal Krebs-Ringer solution, (2) contract the specimen by increasing the KCl to 80 mM for 15 min, and (3) relax the specimen by washing out the bath with normal Krebs-Ringer solution for 10 min. Pilot studies revealed that the order of loading did not affect the results. Unloaded values of wall thickness were acquired using a dissecting microscope on specimens imaged outside the testing chamber; loaded values of thickness were obtained online with the OCT device, with reported values calibrated based on measurements of unloaded thickness using both the higher accuracy microscope and the OCT device.

Data Analysis. Pressure–diameter–thickness and axial force–length data were reported in terms of mean (i.e., transmurally averaged) stress and stretch. The former represent well the actual stress field in homeostatic arteries because residual stresses tend to homogenize the transmural gradient; the latter complement well the values of stress used in the analysis. The mean values of the in-plane Cauchy stresses were thus calculated as

$$\sigma_\vartheta = \frac{P(a_o - h)}{h}, \quad \sigma_z = \frac{f_T + P\pi(a_o - h)^2}{\pi\left((a_o)^2 - (a_o - h)^2\right)}$$

where a_o is the deformed outer radius (with diameter $d_o = 2a_o$), h is the deformed wall thickness, f_T is the axial force measured by the force transducer, and P is the distending (luminal) pressure. Associated mean values of wall stretch were calculated as

$$\lambda_\vartheta = \frac{d_o + (d_o - 2h)}{D_o + (D_o - 2H)}, \; \lambda_z = \frac{l}{L}$$

where D_o is the unloaded outer diameter, H is the undeformed wall thickness, and l and L are the loaded and unloaded axial lengths, respectively.

All data are presented as mean ± standard error of the mean. Two-sample (unpaired) t-tests were used and $p < 0.05$ was considered significant.

Results

Unloaded passive dimensions of the DTA were similar between the two groups, with $n = 5$ (mice) per group. Unloaded outer diameter (D_o) was 818±10 μm for the *Fbln5*$^{+/+}$ group and 838±19 μm for the *Fbln5*$^{-/-}$ group; unloaded wall thickness was 102±5 μm for the *Fbln5*$^{+/+}$ group and 112±2 μm for the *Fbln5*$^{-/-}$ group; and excised length was 5.1±0.1 mm for the *Fbln5*$^{+/+}$ group and 4.5±0.2 mm for the *Fbln5*$^{-/-}$ group. Exposure of mounted, pressurized, and axially stretched specimens to 80 mM K^+ resulted in marked (visible) contractions in both genotypes, but especially in the control mice (Fig. 1).

Contraction-induced changes in outer diameter, axial force, and wall thickness differed quantitatively, but not qualitatively, between the two groups. Illustrative time-course results for both groups studied at 90 mmHg and the three different genotype-specific values of axial stretch are shown in Fig. 2 (*Fbln5*$^{+/+}$ on the left and *Fbln5*$^{-/-}$ on the right). Isobaric contractility, as evidenced by the time-dependent decrease in outer diameter upon exposure to high K^+, was markedly diminished in fibulin-5 deficient vessels at all axial stretches (Fig. 2, top panels). The associated rates at which outer diameter decreased during isobaric contraction and increased upon washout of the K^+ were quantified well by fitting individual segments of the time-course data with a three-parameter exponential function at each axial stretch: $d_o(t) = \bar{d}_o e^{-t/\tau} + d_\infty$. Comparison of best-fit values of the time constants τ revealed no significant differences between the two groups during either contraction or relaxation at 90 mmHg (data not shown). Overall recovery of baseline diameter following washout was nevertheless better in control than *Fbln5*$^{-/-}$ vessels (Fig. 2, top panels), which did not return completely to a baseline diameter.

We found, for the first time, that the transducer-measured contribution to axial force in *Fbln5*$^{+/+}$ control DTAs tended to increase, remain nearly the same, or decrease when the vessels were contracted at fixed values of axial stretch that were increased from below to above the passive preferred in vivo value (Fig. 2, middle panels). Indeed, constancy of force during isobaric contraction occurred at a value of axial stretch just above the preferred passive value in these vessels. This observation suggests that there may exist a "preferred active" value of axial stretch that is favorable mechanically during contraction. A similar, but much diminished, response was seen in the *Fbln5*$^{-/-}$ vessels. Finally, OCT measurements confirmed near isochoric motions via wall thickening during isobaric, axially isometric contractions (Fig. 2,

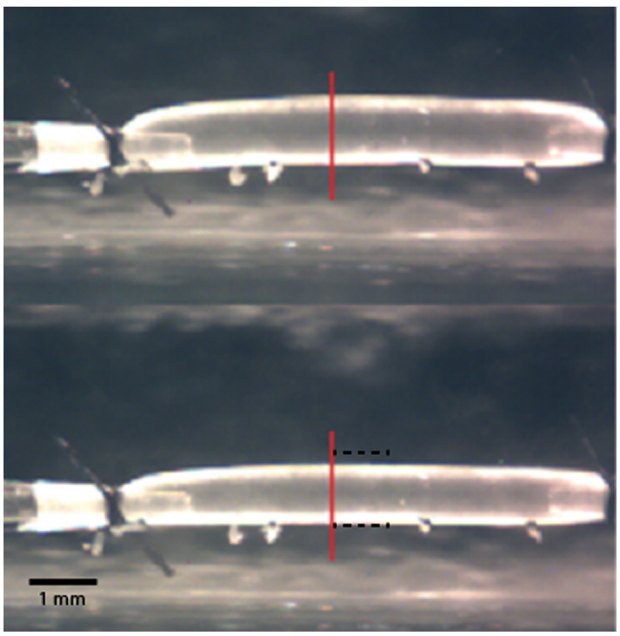

Fig. 1 Illustrative images captured with the video microscope of a *Fbln5*$^{+/+}$ descending thoracic aorta (DTA) loaded at 90 mmHg and an axial stretch of $\lambda_z = 1.5$ both before (top) and after (bottom) 15 min of exposure to 80 mM KCl. Similar, though diminished, responses were observed in *Fbln5*$^{-/-}$ specimens. The vertical line shows the region where outer diameter and wall thickness were measured; the horizontal dashed lines in the bottom image represent the outer diameter before exposure to high KCl. Note the ligated intercostal branches as well as the glass cannulae and ligatures used to secure the sample.

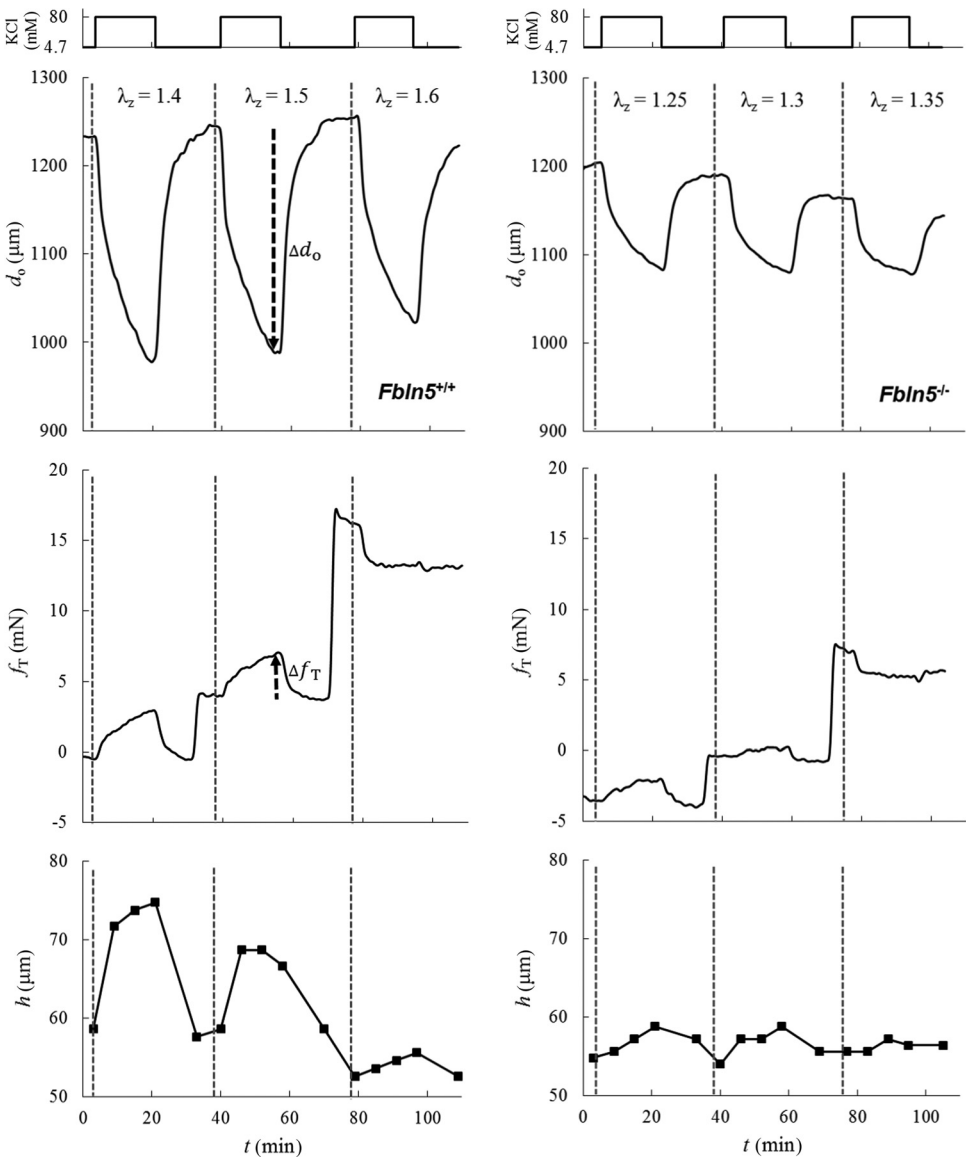

Fig. 2 Illustrative time courses of change in outer diameter measured with the video microscope (d_o—top panels), axial force measured by the force transducer (f_T—middle panels), and wall thickness measured with the OCT (h—bottom panels), all when contracted with 80 mM KCl at 90 mmHg for *Fbln5*$^{+/+}$ (left) and *Fbln5*$^{-/-}$ (right) DTAs at genotype-specific values of axial stretch: $\lambda_z = 1.40$, 1.50, and 1.60 for *Fbln5*$^{+/+}$ and $\lambda_z = 1.25$, 1.30, and 1.35 for *Fbln5*$^{-/-}$. Recall that contraction was maintained at each condition for ~15 min prior to a wash-out with normal Krebs solution. The vertical dashed lines delineate changes in the different fixed values of axial stretch; the dark dashed arrows illustrate, for a single case, the magnitude and direction of contraction-induced changes in outer diameter and axial force that are considered in Fig. 3.

bottom panels). Wall thickening was, therefore, much less in the *Fbln5*$^{-/-}$ vessels in parallel with the diminished decrease in diameter.

Maximal changes, similar to those in Fig. 2 but for all nine conditions (three distending pressures at three different fixed axial stretches), are summarized in Fig. 3 for both groups ($n = 5$ each). For convenience, results are shown as changes from the baseline outer diameter (Δd_o—in microns) and transducer-measured axial force (Δf_T—in millinewtons) after 15 min of contraction with 80 mM KCl (e.g., dark dashed arrows in Fig. 2). Because the fibulin-5 deficient vessels were tested at lower axial stretches, the associated data appear to the left (dashed lines) of the data for the control vessels (solid lines) in Fig. 3. Plotted in this way, it is evident that the reduced isobaric contractility observed in Fig. 2 for the *Fbln5*$^{-/-}$ DTAs, here indicated by Δd_o, existed at all axial stretches at both 70 and 90 mmHg (Fig. 3, top panel). Interestingly, contractility was similarly modest for the two groups at 110 mmHg in terms of both diameter change and axial force generation.

Plotting the change in axial force relative to baseline, that is, Δf_T, versus the isometric axial stretch after 15 min of isobaric contraction for all nine states confirmed (Fig. 3, bottom panel) a genotype-specific "active in vivo axial stretch" (λ_z^{aiv}), which appears to be mechanically favorable. That is, there was no change in axial force upon contraction at this value of axial stretch independent of the level of constant pressure. By fitting a second-order polynomial function to the $\Delta f_T - \lambda_z$ behavior for each fixed value of pressure, interpolated values (i.e., roots) were $\lambda_z^{aiv} = 1.56 \pm 0.01$ for *Fbln5*$^{+/+}$ mice and $\lambda_z^{aiv} = 1.31 \pm 0.01$ for *Fbln5*$^{-/-}$ mice. Interestingly, the change in outer diameter at the genotype-specific values of λ_z^{aiv} was yet reduced significantly in *Fbln5*$^{-/-}$ vessels at 70 and 90 mmHg compared with *Fbln5*$^{+/+}$ vessels when using the same interpolation approach for the $\Delta d_o - \lambda_z$ data

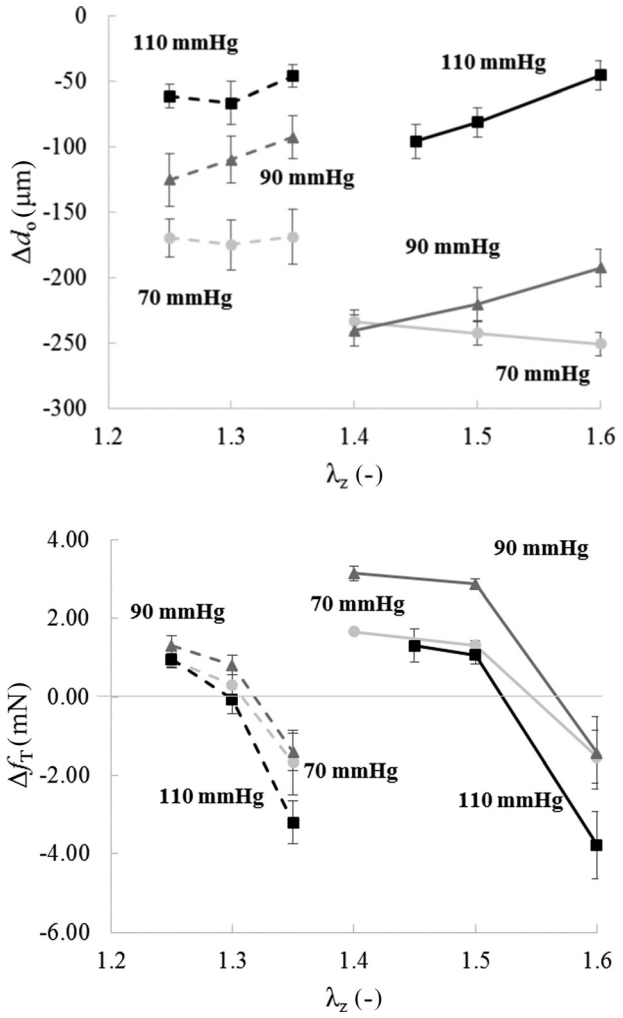

Fig. 3 Changes, relative to genotype-specific baseline values, in outer diameter (Δd_o—top) and axial force (Δf_T—bottom) after 15 min of high K^+ contraction at 70 (circle), 90 (triangle), and 110 (square) mmHg and different values of axial stretch: $\lambda_z = 1.25$, 1.30, and 1.35 for *Fbln5*$^{-/-}$ (dashed line) and $\lambda_z = 1.40-1.45$, 1.50, and 1.60 for *Fbln5*$^{+/+}$ mice (solid line)

(Table 1). This overall finding confirms the illustrative result in Fig. 2 of a diminished change in outer diameter during contraction in fibulin-5 deficiency.

Only small differences were observed between *Fbln5*$^{+/+}$ and *Fbln5*$^{-/-}$ DTAs in the mean circumferential Cauchy stress, in both contracted and relaxed states, when computed at the same pressures but genotype-specific axial stretches. Toward this end, recall that the imposed changes in axial stretch were purposely prescribed to be modest, less than 7% from the intermediate value, to avoid possible damage to the SMCs, especially due to overstretching. The primary change in biaxial stress during isobaric, axially isometric contraction was a decrease in the mean circumferential stress due to a decrease in circumferential stretch, which was consistent in both groups. Only a slightly stiffer behavior was observed via the passive circumferential Cauchy stress (σ_ϑ^{pas})—stretch (λ_ϑ^{pas}) relationship in the *Fbln5*$^{-/-}$ group over the pressure range considered, and total (i.e., contracted) circumferential Cauchy stress (σ_ϑ^{tot})—stretch (λ_ϑ^{tot}) relationships were similar for the two groups. Contraction-induced changes in circumferential stress ($\Delta\sigma_\vartheta$) and stretch ($\Delta\lambda_\vartheta$), calculated by subtracting from the total stress and stretch (σ_ϑ^{tot}, λ_ϑ^{tot}) the corresponding passive values (σ_ϑ^{pas}, λ_ϑ^{pas}), were significantly different in the two groups, however (Fig. 4), again reflecting diminished active changes with fibulin-5 deficiency.

Only small changes were observed in axial Cauchy stress due to contraction ($\Delta\sigma_z$), consistent with a prior study that used a different method of loading during contraction [12]. The total axial stress (σ_z^{tot}), at genotype-specific values of λ_z^{aiv}, was significantly lower in the *Fbln5*$^{-/-}$ group, however (Table 2).

Discussion

Far greater attention is traditionally given to passive properties when studying the mechanics of elastic arteries [3,13], yet a complete understanding of arterial function also requires information on effects of SMC contractility. In most cases when contractility is studied, data are collected using either a ring or a pressure myograph. In the former, an arterial ring is contracted while held at different fixed uniaxial extensions; in the latter, a cylindrical segment is maintained at its presumed in vivo length and contracted at different fixed pressures. Ring tests do not maintain or measure axial extensions or associated forces and thus do not reflect in vivo conditions. Simple pressurization tests replicate in vivo loading conditions, but typically do not provide data on possible changes in axial force due to SMC contraction. Given the importance of biaxial mechanical properties in general [13], there is a need to study effects of contractility on both circumferential and axial behaviors, including biaxial stresses [14].

One of the primary findings of this study is that axial force is not only generated during isobaric, axially isometric contractions of the normal murine descending thoracic aorta, and its value increases, remains nearly the same, or decreases with contraction depending on the particular value of fixed axial stretch independent of the change in outer diameter. That is, the present results suggest that there is a preferred value of axial stretch at which (transducer measured) the axial force does not change with contraction, nearly independent of the level of pressure over the modest range studied herein. Existence of a preferred value of "active in vivo stretch" is reminiscent of the long known existence under passive conditions of a unique value of axial stretch at which (transducer measured) the axial force does not change with pressurization [15]. As noted by Dobrin et al. [16], and confirmed by many others since, such a value of axial stretch appears to be energetically favorable for there is no need for the vessel to perform mechanical work axially to maintain its length during normal excursions of pressure over a cardiac cycle. Importantly, the preferred value of axial stretch, measured under passive conditions, appears to change with adaptations to hemodynamic loads and genetic mutations, and thus can be a good indicator of vessel functionality [17]. The preferred value of axial stretch observed herein in control vessels under active conditions (1.56) was slightly higher than that measured under passive conditions (1.50; see Ref. [3]), which is consistent with a previous anecdotal observation [18].

Table 1 Values of the active in vivo axial stretch λ_z^{aiv} and associated interpolated values for contraction-induced changes in outer diameter Δd_o at λ_z^{aiv} for *Fbln5*$^{+/+}$ and *Fbln5*$^{-/-}$ DTAs at 70, 90, and 110 mmHg

	λ_z^{aiv}	Δd_o (μm) 70 mmHg	Δd_o (μm) 90 mmHg	Δd_o (μm) 110 mmHg
Fbln5$^{+/+}$	156 ± 0.01	−254 ± 5	201 ± 12	67 ± 13
Fbln5$^{-/-}$	131 ± 0.01[a]	170 ± 18[a]	97 ± 17[a]	66 ± 15

[a]$p < 0.05$ between *Fbln5*$^{+/+}$ and *Fbln5*$^{-/-}$.

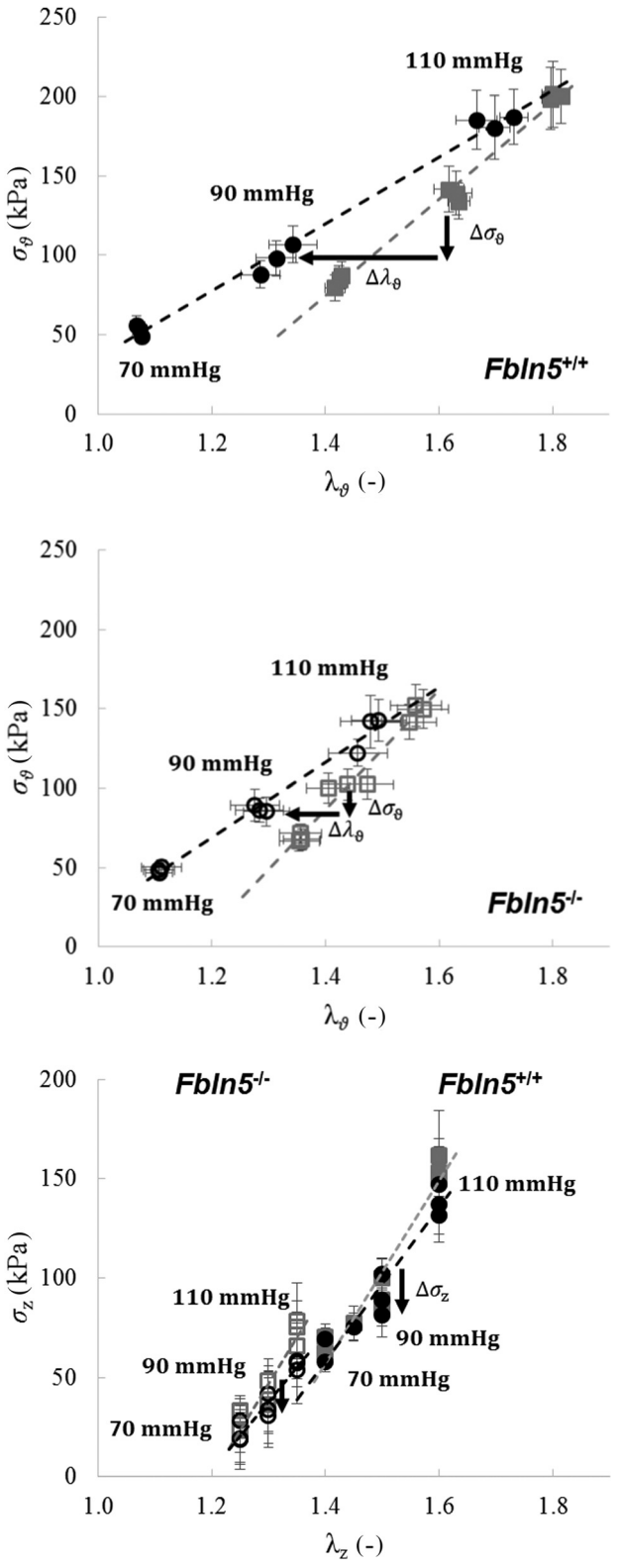

Fig. 4 Circumferential (top and middle) and axial (bottom) Cauchy stress–stretch relationships for both the contracted (black circle) and relaxed (gray square) states for *Fbln5*$^{+/+}$ (solid symbols) and *Fbln5*$^{-/-}$ (open symbols) groups and at the studied pressures and axial stretches. The direction of changes in Cauchy stresses ($\Delta\sigma_\vartheta, \Delta\sigma_z$) and stretch ($\Delta\lambda_\vartheta$) due to isobaric and axially isometric contraction are marked with black arrows.

A second major finding is that fibulin-5 deficiency results in a reduced value of the preferred active in vivo stretch (hence, the reason why the two groups were tested at different axial stretches) as well as significantly diminished contractile responses at isobaric pressures of 70 and 90 mmHg. Nevertheless, some of the general characteristic behaviors of biaxial contractility, including the time course of contraction and relaxation, appeared similar between the *Fbln5*$^{+/+}$ and *Fbln5*$^{-/-}$ groups. The active in vivo axial stretches in *Fbln5*$^{+/+}$ (1.56) and *Fbln5*$^{-/-}$ (1.31) groups were also comparable to the correspondingly different values of in vivo axial stretch in the passive state ($\lambda_z^{iv} = 1.50$ in *Fbln5*$^{+/+}$ and $\lambda_z^{iv} = 1.39$ in *Fbln5*$^{-/-}$; see Ref. [3]); this finding suggests that passive properties may help to organize active properties. However, the $\lambda_z^{aiv} > \lambda_z^{iv}$ in the *Fbln5*$^{+/+}$ vessels resulted in an increase in axial force ($\Delta f_T > 0$) when contracted at λ_z^{iv}, which implies an attempt to retract axially. Conversely, the $\lambda_z^{aiv} < \lambda_z^{iv}$ in the *Fbln5*$^{-/-}$ vessels resulted in a decrease in axial force ($\Delta f_T < 0$) when contracted at the passive value, which implies an attempt to expand axially. Different relationships between the passive in vivo axial stretch λ_z^{iv} and active in vivo axial stretch λ_z^{aiv} may reflect differential interactions between the extracellular matrix and SMC, which are mediated by multiple constituents including elastic fibers [7]. Alternatively, these differences may relate to differences in wall thickness in the two groups and the ability of contraction to thicken the wall further since the observed near incompressibility couples changes in diameter, length, and thickness. The present macroscopic data do not permit any mechanistic interpretation, however.

Although the degree of contractility, as measured by a change in outer diameter during isobaric, axially isometric contraction, was significantly diminished in the *Fbln5*$^{-/-}$ vessels compared with the *Fbln5*$^{+/+}$ vessels at 70 and 90 mmHg, differences were much less at 110 mmHg. It is not clear why the behaviors were similarly modest at the higher pressure, but we emphasize that the prescribed values of pressure were transmural (due to the in vitro setup). In vivo values of transmural pressures are necessarily less than intraluminal pressures because of constraining effects of perivascular tissues [19]. Our focus on the range 70–90 should thus be relevant to normal in vivo transmural pressures where mean luminal pressures are often ~93 mmHg. Interestingly, vessels from *Fbln5*$^{+/+}$ mice displayed an optimal ability to reduce outer diameter via contraction at a transmural pressure near 90 mmHg; this optimal ability was not observed in *Fbln5*$^{-/-}$ specimens. The measured contractility also depended on the applied axial stretch. Contraction-induced changes in outer and inner diameters (using the wall thickness data) decreased significantly ($p < 0.05$) in vessels from *Fbln5*$^{+/+}$ mice contracted at 90 versus 110 mmHg over the range of axial stretches from 1.4 to 1.6. A similar trend was reported in carotid arteries contracted with 90 mM KCl at axial stretches from 1.4 to 1.8 [20], where the in vivo axial stretch in the passive state has been reported to be 1.72 [10]. A better understanding of circumferential–axial coupling in stretch-dependent contractility will likely require a theoretical analysis, however.

The findings illustrated in Fig. 2 suggest that the contractile dysfunction in the *Fbln5*$^{-/-}$ group relates mainly to the magnitude, not the rate, of contraction. Such findings could be related to the number of SMCs or the ability of the SMCs to transmit force to the surrounding extracellular matrix. The latter possibility is consistent with a possible decrease in connections through the elastic fibers in the *Fbln5*$^{-/-}$ mice, particularly in the outer media where mutation tends to affect the fibers [1,3]. Our measurements do not allow us to delineate radially dependent effects. Prior studies of the microstructural composition of the aortic wall did not indicate any significant change in smooth muscle area fraction in *Fbln5*$^{-/-}$ DTAs [3], but a more detailed assessment of potential differences in smooth muscle markers (e.g., SM α-actin, calponin, SM myosin heavy chain, and caldesmon) between *Fbln5*$^{+/+}$ and *Fbln5*$^{-/-}$ aortas would obviously provide additional insight into the dysfunction observed at the vessel level.

Table 2 Interpolated values of the total (contracted) circumferential stretch and biaxial Cauchy stresses based on data collected at 90 mmHg at λ_z^{aiv} for *Fbln5*$^{+/+}$ and *Fbln5*$^{-/-}$ DTAs. No significant difference in circumferential stress and stretch was found between the two groups though there was a significant difference in activation-induced change in stress during SMC contraction. The total axial stress was significantly different between the two groups while changes during contraction were small.

	λ_ϑ^{tot}	$\Delta\lambda_\vartheta$	σ_ϑ^{tot} (kPa)	$\Delta\sigma_\vartheta$ (kPa)	σ_z^{tot} (kPa)	$\Delta\sigma_z$ (kPa)
Fbln5$^{+/+}$	1.33 ± 0.04	− 0.29 ± 0.02	106.4 ± 11.04	−33.8 ± 5.3	123.7 ± 8.1	−9.2 ± 3.7
Fbln5$^{-/-}$	1.28 ± 0.04	− 0.14 ± 0.02[a]	89.4 ± 9.4	−12.1 ± 2.8[a]	41.0 ± 15.0[a]	−6.1 ± 2.0

[a]$p < 0.05$ between *Fbln5*$^{+/+}$ and *Fbln5*$^{-/-}$.

Male mice were used in this study. Vessel-level contractile responses, due to depolarization by KCl, of thoracic aortic rings from C57BL/6 mice previously revealed similar responses between male and female mice [21], and is consistent with our previous findings of similar passive properties in male and female control and fibulin-5 deficient mice [3].

Whereas vessel-level contractility is fundamental to flow regulation by muscular arteries and arterioles, it is not clear what role contractility plays in elastic arteries whose primary mechanical function is to store and use elastic energy to augment blood flow. Indeed, it seems that aortic SMCs may be responsible primarily for sensing and regulating the extracellular matrix of the media to ensure appropriate compliance, not contractility. Nevertheless, contraction of circumferentially oriented SMCs could contribute to the mechanical integrity or stability of the vessel wall [22]. Indeed, the simple analysis of mean wall stresses presented herein confirms prior computational simulations [23] that vascular SMC contraction can reduce biaxial stresses at a fixed pressure and axial stretch, mainly by increasing the wall thickness and reducing the luminal diameter, which in turn reduces circumferential stretch (Fig. 4). This finding was consistent in both genotypes. Hence, despite the reduced contractility in the *Fbln5*$^{-/-}$ DTAs, a potentially protective function of reducing circumferential stress by contraction was maintained. Indeed, the magnitude of the total circumferential stress and stretch was similar in both groups in the contracted state despite the contractile range being significantly lower in the *Fbln5*$^{-/-}$ group compared with the *Fbln5*$^{+/+}$ group. This finding suggests a cooperative relationship between active and passive properties in the wall, with the degree of axial stretch being fundamental to all aspects of the wall mechanics. This finding may also imply a relationship between vessel-level contractility and wall thickness. The reduced ability of the *Fbln5*$^{-/-}$ aorta to increase its wall thickness through contraction (Fig. 2) may have been compensated by an increased overall passive wall thickness [3].

Notwithstanding the importance of the biaxial mechanics of contractility, there have been but a few prior experimental studies (e.g., Refs. [14,24]) and only one careful study in the mouse aorta. Agianniotis et al. [12] reported standard cyclic pressure–diameter testing, at multiple values of fixed axial stretch, of an unspecified region of the thoracic aorta in C57BL/6 wild-type mice. Their primary finding was that the contracted artery develops a nonmonotonic active axial stress—axial stretch response that is virtually independent of the value of pressure. This Frank–Starling-like response suggests that there is a value of axial stretch at which the vessel can generate a maximum value of axial stress. Interestingly, this maximum occurred at an axial stretch that was slightly higher than the preferred value of axial stretch measured under passive conditions. Our results for the control mice are similar to theirs. Yet, differences between the two studies include their use of a different strain of mouse (a pure C57BL/6), the vasoconstrictor phenylephrine to contract the vessels, continuous pressure loading (from 0 to 150 mmHg) of contracted vessels (similar to Ref. [14], who otherwise used lower values of maximum pressures), and larger values of axial stretch. Their values of axial stretch are closer to those we reported previously for the ascending thoracic aorta [3], but it is not clear whether they tested the ascending or descending segment. Whereas continuous pressure loading experiments are clearly useful, particularly from the perspective of traditional biomechanical constitutive modeling, we preferred isobaric, axially isometric loading herein for two reasons. First, unlike the heart, arteries do not experience a full range of pressures from zero to physiologic; hence, isobaric pressures within the range 70–110 mmHg modeled better the mean pressures that are experienced in vivo. Second, from the perspective of thermomechanics, it is useful to maintain constant all state variables but one during experimentation [25]. Since the state of SMC contractility changed during K^+ loading as the ions diffused into the wall and generated a time course of changes in diameter and axial force (cf. Fig. 2), we maintained constant both pressure and axial stretch at multiple combinations. Albeit beyond the scope of the current paper, such data should prove useful in modeling SMC contractility within the framework of a chemomechanical model (cf. Refs. [26–28]). Indeed, given the current findings of differential biomechanical responses of smooth muscle in control and fibulin-5 deficient mice, a more detailed pharmacological and biological study is now warranted.

In particular, it is not known whether changes in the mechanical properties of the extracellular matrix trigger adaptations in vascular SMC contractility, or vice versa. Prior data suggest that passive material stiffness is not different due to fibulin-5 deficiency [3]; yet, we found a diminished contractility in the *Fbln5*$^{-/-}$ aortas. Hence, although the present data suggest that there is a strong relationship between passive and active axial behaviors in the normal and mutant vessels, the coupled biaxial nature of these relationships is clearly complex. Again, further insight will likely require a detailed chemomechanical model of the vessel. One hypothesis that should be tested is a potentially protective role of maintaining passive material stiffness in the face of diminished vessel-level contractility.

In summary, the present data suggest that there is a value of axial stretch at which contraction-induced changes in diameter do not elicit any change in axial force. This preferred value of axial stretch is comparable to previously measured values in the passive state, but slightly higher in normal vessels. Preliminary results suggested that this "active in vivo stretch" did not change as a function of the degree of actomyosin activity (e.g., calcium-dependent activation of smooth muscle myosin). Indeed, the significantly reduced value of this stretch in fibulin-5 deficiency was likely part of an overall adaptive process that similarly reduced the passive in vivo stretch, which in turn appeared to preserve the passive material stiffness [3]. The present data show further that fibulin-5 deficiency results in a markedly diminished contractile response, particularly at pressures within the expected physiologic range of transmural pressures, 70–90 mmHg. Given that reduced contractility is thought to play a role in TAADs [7,29], and yet *Fbln5*$^{-/-}$ mice that exhibit a severe aortic elastopathy do not develop these lesions [1,3], there is a pressing need for similar studies in mouse models that predispose to aneurysms or dissections to try, via comparative studies, to elucidate specific mechanisms by which altered contractility may play a role in these potentially lethal conditions [30].

Acknowledgment

This research was supported, in part, by a grant from the U.S. NIH (R01 HL105297) and by a Grant (#2012419) from the Swedish Research Council.

References

[1] Yanagisawa, H., Davis, E. C., Starcher, B. C., Ouchi, T., Yanagisawa, M., Richardson, J. A., and Olson, E. N., 2002, "Fibulin-5 is an Elastin-Binding Protein Essential for Elastic Fiber Development In Vivo," Nature, **415**(6868), pp. 168–171.

[2] Le, V. P., Cheng, J. K., Kim, J., Staiculescu, M. C., Ficker, S. W., Sheth, S. C., Bhayani, S. A., Mecham, R. P., Yanagisawa, H., and Wagenseil, J. E., 2015, "Mechanical Factors Direct Mouse Aortic Remodeling During Early Maturation," J. R. Soc. Interface., **12**(104), p. 20141350.

[3] Ferruzzi, J., Bersi, M. R., Uman, S., Yanagisawa, H., and Humphrey, J. D., "Decreased Energy Storage, Not Increased Material Stiffness, Characterizes Central Artery Dysfunction in Fibulin-5 Deficiency Independent of Sex," ASME J. Biomech. Eng., **137**(3), p. 031007.

[4] Pereira, L., Lee, S. Y., Gayraud, B., Andrikopoulos, K., Shapiro, S. D., Bunton, T., Biery, N. J., Dietz, H. C., Sakai, L. Y., and Ramirez, F., 1999, "Pathogenetic Sequence for Aneurysm Revealed in Mice Under Expressing Fibrillin-1," Proc. Natl. Acad. Sci. USA, **96**(7), pp. 3819–3823.

[5] Huang, J., Davis, E. C., Chapman, S. L., Budatha, M., Marmorstein, L. Y., Word, R. A., and Yanagisawa, H., 2010, "Fibulin-4 Deficiency Results in Ascending Aortic Aneurysms: A Potential Link Between Abnormal Smooth Muscle Cell Phenotype and Aneurysm Progression," Circ. Res., **106**(3), pp. 583–592.

[6] Wang, X., LeMaire, S. A., Chen, L., Carter, S. A., Shen, Y. H., Gan, Y., Bartsch, H., Wilks, J. A., Utama, B., Ou, H., Thompson, R. W., Coselli, J. S., and Wang, X. L., 2005, "Decreased Expression of Fibulin-5 Correlates With Reduced Elastin in Thoracic Aortic Dissection," Surgery, **138**(2), pp. 352–359.

[7] Humphrey, J. D., Schwartz, M. A., Tellides, G., and Milewicz, D. M., 2015, "Role of Mechanotransduction in Vascular Biology: Focus on Thoracic Aortic Aneurysms and Dissections," Circ. Res., **116**(8), pp. 1448–1461.

[8] Kim, H. R., Appel, S., Betterkind, S., Gangopadhyay, S. S., and Morgan, K. G., 2008, "Smooth Muscle Signaling Pathways in Health and Disease," J. Cell. Mol. Med., **12**(6a), pp. 2165–2180.

[9] Putz, S., Lubomirov, L. T., and Pfitzer, G., 2009, "Regulation of Smooth Muscle Contraction by Small GTPases," Physiology, **24**(6), pp. 324–356.

[10] Ferruzzi, J., Bersi, M. R., and Humphrey, J. D., 2013, "Biomechanical Phenotyping of Central Arteries in Health and Disease: Advantages of and Methods for Murine Models," Ann. Biomed. Eng., **41**(7), pp. 1311–1330.

[11] Gleason, R. L., Gray, S. P., Wilson, E., and Humphrey, J. D., 2004, "A Multiaxial Computer-Controlled Organ Culture and Biomechanical Device for Mouse Carotid Arteries," ASME J. Biomech. Eng., **126**(6), pp. 787–795.

[12] Agianniotis, A., Rachev, A., and Stergiopulos, N., 2012, "Active Axial Stress in Mouse Aorta," J. Biomech., **26**(45), pp. 1924–1927.

[13] Humphrey, J. D., 2002, *Cardiovascular Solid Mechanics: Cells, Tissues, and Organs*, Springer, New York.

[14] Wagner, H. P., and Humphrey, J. D., 2011, "Differential Passive and Active Biaxial Mechanical Behaviors of Muscular and Elastic Arteries: Basilar Versus Common Carotid," ASME J. Biomech. Eng., **133**(5), p. 051009.

[15] Van Loon, P., Klip, W., and Bradley, E. L., 1977, "Length-Force and Volume–Pressure Relationships of Arteries," Biorheology, **14**(4), pp. 181–201.

[16] Dobrin, P. B., Schwarcz, T. H., and Mrkvicka, R., 1990, "Longitudinal Retractive Force in Pressurized Dog and Human Arteries," J. Surg. Res., **48**(2), pp. 116–120.

[17] Humphrey, J. D., Eberth, J. F., Dye, W. W., and Gleason, R. L., 2009, "Fundamental Role of Axial Stress in Compensatory Adaptations by Arteries," J. Biomech., **42**(1), pp. 1–8.

[18] Dye, W. W., Gleason, R. L., Wilson, E., and Humphrey, J. D., 2007, "Altered Biomechanical Properties of Carotid Arteries in Two Mouse Models of Muscular Dystrophy," J. Appl. Physiol., **103**(2), pp. 664–672.

[19] Humphrey, J. D., and Na, S., 2002, "Elastodynamics and Arterial Wall Stress," Ann. Biomed. Eng., **30**(4), pp. 509–523.

[20] Zulliger, M. A., Kwak, N. T., Tsapikouni, T., and Stergiopulos, N., 2002, "Effects of Longitudinal Stretch on VSM Tone and Distensibility of Muscular Conduit Arteries," Am. J. Physiol. Heart Circ. Physiol., **283**(6), pp. H2599–H2605.

[21] Knapp, J., Aleth, S., Balzer, F., Gergs, U., Schmitz, W., and Neumann, J., 2006, "Comparison of Contractile Responses in Isolated Mouse Aorta and Pulmonary Artery: Influence of Strain and Sex," J. Cardiovasc. Pharmacol., **48**(1), pp. 820–826.

[22] Cyron, C., and Humphrey, J. D., 2015, "Preferred Fiber Orientations in Healthy Arteries and Veins Understood from Netting Analysis," Math. Mech. Solids., **20**(6), pp. 680–696.

[23] Humphrey, J. D., and Wilson, E., 2003, "A Potential Role of Smooth Muscle Tone in Early Hypertension: A Theoretical Study," J. Biomech., **36**(11), pp. 1595–1601.

[24] Takamizawa, K., Hayashi, K., and Matsuda, T., 1992, "Isometric Biaxial Tension of Smooth Muscle in Isolated Cylindrical Segments of Rabbit Arteries," Am. J. Physiol., **263**(1), pp. H30–H34.

[25] Humphrey, J. D., 2003, "Continuum Thermomechanics and the Treatment of Disease and Injury," ASME Appl. Mech. Rev., **56**(2), pp. 231–260.

[26] Murtada, S. -I., Kroon, M., and Holzapfel, G. A., 2010, "A Calcium-Driven Mechanochemical Model for Prediction of Force Generation in Smooth Muscle," Biomech. Model. Mechanobiol., **9**(6), pp. 749–762.

[27] Murtada, S.-I., Arner, A., and Holzapfel, G. A., 2012, "Experiments and Mechanochemical Modeling of Smooth Muscle Contraction: Significance of Filament Overlap," J. Theor. Biol., **297**, pp. 176–186.

[28] Murtada, S. -I., Lewin, S., Arner, A., and Humphrey, J. D., "Adaptation of Active Tone in the Mouse Descending Thoracic Aorta Under Acute Changes in Loading," Biomech. Model. Mechanobiol. (in press).

[29] Milewicz, D. M., Gou, D. C., Fadulu, V. T., Lafont, A. L., Papke, C. L., Inamoto, S., Kwartler, C. S., and Pannu, H., 2008, "Genetic Basis of Thoracic Aortic Aneurysms and Dissections: Focus on Smooth Muscle Cell Contractile Dysfunction," Annu. Rev. Genomics. Hum. Genet., **9**(1), pp. 283–302.

[30] Ferruzzi, J., Murtada, S.-I., Li, G., Jiao, Y., Uman, S., Ting, M. Y.-L., Tellides, G., and Humphrey, J. D., 2016, "Pharmacologically Improved Contractility Protects Against Aortic Dissection in Mice With Disrupted TGFb Signaling Despite Compromised ECM Properties," Arterioscl. Thromb. Vasc. Biol. (in press).